Carbohydrate Polymers 319 (2023) 121187

Contents lists available at ScienceDirect

Carbohydrate Polymers

journal homepage: www.elsevier.com/locate/carbpol

Type of intrinsic resistant starch type 3 determines *in vitro* fermentation by pooled adult faecal inoculum

C.E. Klostermann [a,b], M.F. Endika [c], E. ten Cate [a,b], P.L. Buwalda [a,d,†], P. de Vos [e], J.H. Bitter [a], E.G. Zoetendal [c], H.A. Schols [b,*]

[a] *Biobased Chemistry and Technology, Wageningen University & Research, Bornse Weilanden 9, 6708 WG Wageningen, the Netherlands*
[b] *Laboratory of Food Chemistry, Wageningen University & Research, Bornse Weilanden 9, 6708 WG Wageningen, the Netherlands*
[c] *Laboratory of Microbiology, Wageningen University & Research, Stippeneng 4, 6708 WE Wageningen, the Netherlands*
[d] *Coöperatie Koninklijke AVEBE u.a., P.O. Box 15, 9640 AA Veendam, the Netherlands*
[e] *Immunoendocrinology, Division of Medical Biology, Department of Pathology and Medical Biology, University of Groningen and University Medical Centre Groningen, Groningen, Hanzeplein 1, 9700 RB Groningen, the Netherlands*

ARTICLE INFO

Keywords:
Butyrate
Microbiota
Dietary fibre
Crystal type
Molecular weight distribution

ABSTRACT

Resistant starch (RS) results in relatively high health-beneficial butyrate levels upon fermentation by gut microbiota. We studied how physico-chemical characteristics of RS-3 influenced butyrate production during fermentation. Six highly resistant RS-3 substrates (intrinsic RS-3, 80–95 % RS) differing in chain length (DPn 16–76), Mw distribution (PI) and crystal type (A/B) were fermented *in vitro* by pooled adult faecal inoculum. All intrinsic RS-3 substrates were fermented to relatively high butyrate levels (acetate/butyrate $\leq$ 2.5), and especially fermentation of A-type RS-3 prepared from polydisperse α-1,4 glucans resulted in the highest relative butyrate amount produced (acetate/butyrate: 1). Analysis of the microbiota composition after fermentation revealed that intrinsic RS-3 stimulated primarily *Lachnospiraceae*, *Bifidobacterium* and *Ruminococcus*, but the relative abundances of these taxa differed slightly depending on the RS-3 physico-chemical characteristics. Especially intrinsic RS-3 of narrow disperse Mw distribution stimulated relatively more *Ruminococcus*. Selected RS fractions (polydisperse Mw distribution) obtained after pre-digestion were fermented to acetate and butyrate (ratio $\leq$ 1.8) and stimulated *Lachnospiraceae* and *Bifidobacterium*. This study indicates that especially the α-1,4 glucan Mw distribution dependent microstructure of RS-3 influences butyrate production and microbiota composition during RS-3 fermentation.

1. Introduction

Butyrate is a short-chain fatty acid (SCFA) that is among others essential for health by providing energy to colonocytes (Fu, Liu, Zhu, Mou, & Kong, 2019). In addition, butyrate has been associated with modulation of immune and inflammatory responses, stimulation of intestinal barrier function and with prevention of colorectal cancer (Chen & Vitetta, 2018; Cushing, Alvarado, & Ciorba, 2015; Markiewicz, Ogrodowczyk, Wiczkowski, & Wroblewska, 2021; McNabney & Henagan, 2017; Ryu, Kaiko, & Stappenbeck, 2018). To increase butyrate production in the colon and promote a healthy colonic environment, resistant starch (RS) could be a promising fibre to be included in the diet. RS is defined as starch that escapes digestion and arrives in the colon, where it will be fermented by colonic bacteria to SCFAs like acetate, propionate and butyrate. Compared to other dietary fibres, RS is known to be fermented to high amounts of butyrate by gut microbiota (Jonathan et al., 2012; Wang et al., 2019). Five different types of RS exist, of which type 1 and 2 are native starch forms that can be found in plants. Type 3 refers to retrograded starch, produced after gelatinisation and cooling of starch, whereas type 4 is chemically modified starch and type 5 comprises the amylose-lipid complexes (Birt et al., 2013). The fermentability of these 5 types of RS by gut microbiota differs immensely, both between RS types as within an RS type (Giuberti & Gallo, 2020; Gu, Li, Hamaker, Gilbert, & Zhang, 2020; Li et al., 2015; Teichmann & Cockburn, 2021; Zhou, Cao, & Zhou, 2013). Among the different types of RS, resistant starch type 3 is of interest for its thermal stability and

* Corresponding author.
E-mail address: henk.schols@wur.nl (H.A. Schols).
† Deceased.

https://doi.org/10.1016/j.carbpol.2023.121187
Received 28 April 2023; Received in revised form 29 June 2023; Accepted 7 July 2023
Available online 8 July 2023

applicability as food ingredient (Haralampu, 2000).

Fermentation of resistant starch has been associated with increased levels of *Bifidobacterium*, *Ruminococcus* and genera often associated with butyrate production such as *Eubacterium*, *Faecalibacterium* and *Roseburia* (Baxter et al., 2019). It has been shown that *Bifidobacterium adolescentis* and *Ruminococcus bromii* are the species that are mostly responsible for primary degradation of RS, since they express many α-amylases and carbohydrate binding modules (CBMs) that are associated with degradation of insoluble starches (Cerqueira, Photenhauer, Pollet, Brown, & Koropatkin, 2020; Ze, Duncan, Louis, & Flint, 2012). Both *R. bromii* and *B. adolescentis* do not produce butyrate themselves (Laverde Gomez et al., 2019; Pokusaeva, Fitzgerald, & van Sinderen, 2011), but cross-feed with butyrate producing bacteria like *Agathobacter rectalis* (previously known as *Eubacterium rectale*), *Faecalibacterium prausnitzii* and *Roseburia faecis* (Maier et al., 2017). These species use acetate, alone or in combination with lactate, as energy sources resulting in the production of butyrate. This cross-feeding results in an efficient degradation of RS (Ze et al., 2012) and a relatively high production of butyrate (Pryde, Duncan, Hold, Stewart, & Flint, 2002).

Resistant starch type 3 (RS-3) can be produced by gelatinising starch followed by retrogradation. RS-3 is commercially produced from high-amylose starch (Jacobasch, Dongowski, Schmiedl, & Muller-Schmehl, 2006) or long-chain maltodextrin obtained after partial enzymatic debranching of tapioca starch (Scheiwiller, Arrigoni, Brouns, & Amado, 2006). RS-3 can also be produced by controlled crystallisation of debranched amylopectins at specific temperatures to result in either A- or B-type crystals (Cai & Shi, 2014; Klostermann et al., 2021). However, debranching amylopectins results in α-glucans with a quite broad Mw distribution (polydispersity index (PI) > 1.3) (Klostermann et al., 2021). A controlled chain length of α-1,4 glucans can be achieved by the use of synthesising enzymes (Klostermann et al., 2021; Kobayashi, Kimura, Naito, Togawa, & Wada, 2015), resulting in α-1,4 glucans with a more narrow disperse Mw distribution (PI < 1.3). Recently, twelve unique RS-3 preparations differing in Mw, Mw distribution and crystal type were produced, obtained by crystallisation of either debranched amylopectins or enzymatically synthesised α-1,4 glucans (Klostermann et al., 2021). Pancreatic digestion of these twelve RS-3 preparations revealed that especially long chain B-type crystals (DPn 32–76) and short-chain A-type crystals (DPn 15–22) are resistant to digestion by pancreatic α-amylase, with 80–95 % of the starch expected to reach the colon (Klostermann et al., 2021). Since these specific RS-3 preparations do only contain a minor fraction of digestible starch, they are considered as "intrinsic RS" and are quite different from commercial RS-3 ingredients like Novelose® 330 and C*Actistar, that contain up to 50 % RS (Giuberti & Gallo, 2020), and thereby should better be referred to as "RS-rich".

Not many studies focussed on the fermentability of RS-3 *in vitro* and *in vivo*. Only few studies used commercial RS-rich RS-3 ingredients (Giuberti & Gallo, 2020; Plongbunjong, Graidist, Bach Knudsen, & Wichienchot, 2017), used RS-3 preparations from debranched starches produced in a laboratorial setting (Chang et al., 2021; Gu et al., 2020; Liu et al., 2022; Zhang et al., 2021), or produced RS-3 rich starches from raw potatoes (Teichmann & Cockburn, 2021). All these studies thus used RS-3 preparations made of α-glucans with a polydisperse Mw distribution. These studies mentioned the production of SCFAs and changes in microbiota composition during *in vitro* fermentation, but did not include a quantitative analysis on the starch consumption by the gut microbiota. An *in vitro* fermentation study incorporating RS-3 structures with a defined crystal type, Mw and especially Mw distribution is still lacking, but needed to understand which chemical features are responsible for distinct SCFA production by the gut microbiota.

We investigated how RS-3 is fermented by gut microbiota of healthy adults and which RS-3 physico-chemical characteristics influence butyrate production in the colon. To study the butyrogenic potential of novel and well-characterised RS-3 preparations (Klostermann et al., 2021), six intrinsic RS-3 substrates and two RS enriched fractions, obtained after pre-digestion of selected RS-3 preparations, were fermented *in vitro* by an inoculum consisting of a pool of four adult faecal samples. A new sampling method for insoluble fibres was developed to enable quantification of the remaining soluble and insoluble starch during fermentation. Starch degradation, SCFA production and microbiota composition were determined during *in vitro* fermentation. Additionally, the change in morphology of RS-3 particles due to fermentation was analysed over time using scanning electron microscopy (SEM).

2. Materials and methods

2.1. Materials

Medium components used for the *in vitro* fermentation and a dialysate solution containing 25 g/L $K_2HPO_4{\cdot}3H_2O$, 45 g/L NaCl, 0.05 g/L $FeSO_4{\cdot}7H_2O$ and 0.5 g/L ox-bile were obtained from Tritium Microbiologie (Eindhoven, The Netherlands). L-cysteine-hydrochloride, 2-(*N*-morpholino)ethanesulfonic acid (MES), soluble potato starch (SPS) and porcine pancreatin were obtained from Sigma-Aldrich (St. Louis, Missouri, USA).

2.1.1. RS-3 preparations

RS-3 preparations were prepared by crystallisation of α-1,4 glucans obtained by either debranching (enzymatically modified) amylopectins or enzymatic synthesis as described by Klostermann et al. (2021). The (enzymatically modified) amylopectins included waxy potato starch (WPS, Eliane100) and amylomaltase modified potato starch (AMPS, Etenia457) provided by AVEBE (Veendam, The Netherlands) and waxy rice starch (WRS, Remyline XS) obtained from Beneo (Mannheim, Germany). The specific physico-chemical characteristics and *in vitro* digestibility of the obtained RS-3 preparations have been described in detail by Klostermann et al. (2021) and are summarised in Table 1 in the Results section.

2.1.2. Faecal slurry

Faecal material of four healthy adults was collected, after signing a written informed consent. Subjects were between 27 and 35 years old, had a BMI between 19 and 22 kg/m^2, were non-smokers, did not have any health complaints, and did not use antibiotics for over 6 months prior to collection. Faecal samples were stored immediately in a sterile 50 mL container with filter screw cap (Greiner Bio-One CELLSTAR™ tube, Kremsmünster, Austria). The container was placed inside a pouch with a BD GasPak EZ anaerobe gas generating system with indicator (BD Diagnostics, Sparks, Maryland, USA) and stored at 4 °C for a maximum of 24 h until processing. Pooled adult faecal slurry was prepared in an anaerobic chamber (gas composition: 4 % H_2, 15 % CO_2, 81 % N_2, Bactron 300, Sheldon Manufacturing, Cornelius, Oregon, USA) by mixing equal aliquots of fresh faeces with a pre-reduced dialysate-glycerol solution to 25 % *w/v* as previously described (Aguirre et al., 2015). The pre-reduced dialysate-glycerol solution contained ten times diluted dialysate solution, 10 % glycerol, 0.5 mg/L resazurin, 0.4 g/L L-cysteine-hydrochloride, supplemented with 0.45 g/L $CaCl_2{\bullet}2H_2O$ and 0.5 g/L $MgSO_4{\bullet}7H_2O$. The final faecal slurry was snap-frozen using liquid nitrogen and stored at −80 °C prior to use.

2.2. In vitro batch fermentation of RS-3 preparations

2.2.1. Culture medium

The culture medium was based on Simulated Ileal Efflux Medium (SIEM) as described previously (Minekus et al., 1999) with minor modifications and is referred to as mSIEM. The carbohydrate component, pre-mixed from Tritium Microbiologie, was ten times lowered when compared to Minekus et al. (1999) and consisted of pectin, xylan, arabinogalactan, amylopectin (all at 0.048 g/L) and soluble starch (0.4 g/L). The protein component consisted of bactopeptone and casein (both at 3 g/L). Additionally, the medium contained 0.05 g/L ox-bile, 2.5 g/L $K_2HPO_4{\cdot}3H_2O$, 4.5 g/L NaCl, 0.45 g/L $CaCl_2{\cdot}2H_2O$, 0.005 g/L

Table 1
Physico-chemical and digestibility characteristics of RS-3 preparations used in this study as described in Klostermann et al. (2021). DPn (number-based degree of polymerisation) and PI (polydispersity index) were determined using HPSEC-RI, crystal type was determined using XRD and *in vitro* digestion was performed using pancreatin and amyloglucosidase (Klostermann et al., 2021). RS-rich refers to 20–70 % RS and intrinsic RS refers to ≥80 % RS.

Sample name	Reported as[a]	Crystal type	$DPn_{crystal}$	$PI_{crystal}$	*In vitro* digestibility (120 min (%))	RS category
N16-A	sG2-A	A	16	1.23	20	Intrinsic
N18-A	sG5-A	A	18	1.21	12	Intrinsic
P21-A	dWRS-A	A	21	1.59	21	Intrinsic
P22-B	dWRS-B	B	22	1.50	80	RS-rich
N32-B	sG20-B	B	32	1.14	5	Intrinsic
P40-B	dWPS-B	B	40	2.11	26	RS-rich
P53-B	dAMPS-B	B	53	1.67	9	Intrinsic
N76-B	sG65-B	B	76	1.07	6	Intrinsic

[a] Klostermann et al., 2021.

$FeSO_4 \cdot 7H_2O$ and 0.01 g/L haemin, 0.5 g/L $MgSO_4$, and 0.4 g/L L-cysteine-hydrochloride. A vitamin mix was added with a final concentration of 1 μg/L menadione, 2 μg/L D-biotin, 0.5 μg/L vitamin B12, 10 μg/L D-pantothenate, 5 μg/L nicotinamide adenine dinucleotide, 5 μg/L aminobenzoic acid, 4 μg/L thiamine HCl. The medium was buffered at pH 5.8 using 0.1 M MES buffer. The medium was stored overnight in the anaerobic chamber with an opened lid to remove head-space oxygen.

Culture medium containing soluble potato starch (mSIEM + SPS) was prepared by dissolving 40 mg/mL SPS in sterile milliQ (MQ) water in a boiling water bath for 10 min. After cooling, the solubilised SPS was mixed with concentrated mSIEM to obtain a final concentration of 11.11 mg/mL SPS in mSIEM. The final mSIEM + SPS medium was stored overnight in the anaerobic chamber with an opened lid to remove head-space oxygen.

2.2.2. Pre-digestion of RS-3 preparations

Pre-digestion was performed based on methods as previously described by Martens and colleagues (Martens, Gerrits, Bruininx, & Schols, 2018), with 2 mg pancreatin per mg starch. In short, porcine pancreatin solution was prepared by mixing 12 g pancreatin (8 × USP specifications (P7545), Sigma-Aldrich; enzyme was sufficient to theoretically degrade digestible starch in <1 min) in 80 mL MQ head-over-tail for 10 min, followed by centrifugation at 4 °C, 7000 ×*g* for 10 min. The supernatant was collected and an aliquot of 48.8 mL of the supernatant was diluted with 11.2 mL MQ to obtain pancreatin solution. Pancreatin solution (20 %), 0.5 M sodium acetate buffer pH 5.9 (20 %) and MQ were added to RS-3 preparations P40-B, P21-A and P22-B to obtain a suspension of approximately 20 mg/mL in 100 mM sodium acetate buffer pH 5.9 (Klostermann et al., 2021). The suspension was incubated in a shaking incubator at 37 °C, 100 rpm for 6 h. Afterwards, the suspension was centrifuged at 4 °C, 7000 ×*g* for 10 min, and the supernatant was decanted. The remaining pellet was washed 4 times with MQ water, after which the pellet was dried at 40 °C for 48 h. The remaining material was homogenised with a mortar to obtain pre-digested (pd) RS-3 starches P40-B-pd, P21-A-pd and P22-B-pd. To yield P40-B-pd and P21-A-pd, ±23 % and ±18 % of the total starch was digested, respectively, which values are close to the digestible starch fraction reported previously for the undigested starches (Klostermann et al., 2021). For P22-B yielding P22-B-pd, ±47 % of the total starch was digested, which was lower compared to the digestible starch fraction reported previously (Klostermann et al., 2021), indicating that P22-B-pd might still contain a fraction of digestible starch.

2.2.3. In vitro batch fermentation

RS-3 preparations (±20 mg dry weight), either directly or after pre-digestion (Section 2.2.2.), were weighed in duplicate in sterile 5 mL serum bottles for each individual sampling time. The weighed RS-3 preparations were stored overnight in the anaerobic chamber.

In the anaerobic chamber, inoculum was prepared by diluting pooled adult faecal slurry to 10 mg/mL faeces in mSIEM. An aliquot of 1.8 mL mSIEM was added to the serum bottles containing RS-3 preparations and subsequently 0.2 mL inoculum was added. Serum bottles containing mSIEM + SPS were also incubated with inoculum to obtain 10 mg/mL SPS with 1 mg/mL faeces. In addition, substrate blanks (without inoculum) and medium blanks (including mSIEM carbohydrates, without additional substrate) were included. All serum bottles were capped with butyl rubber stoppers. In a first fermentation experiment, intrinsic RS-3 substrates (N16-A, N18-A, P21-A, N32-B, P53-B and N76-B) were incubated at 37 °C, 100 rpm for 0, 24 and 48 h (Section 3.2). In a second fermentation experiment, pre-digested RS-3 preparations (P22-B-pd and P40-B-pd) and controls (N32-B and P21-A-pd) were incubated at 37 °C, 100 rpm for 0, 8, 24, 36 and 48 h (Section 3.3).

To accurately quantify the degradation of insoluble (resistant) starches, a dedicated sampling method was developed. At each time point, the serum bottles were decapped and the insoluble RS-3 preparations were re-suspended. Immediately, 1.8 mL was transferred to sterile weighed Safe-Lock Eppendorf tubes (Eppendorf, Hamburg, Germany). Subsequently, the tubes were centrifuged at 4 °C, 20,000 ×*g* for 10 min and the supernatant was separated from the pellet. The supernatant was heated to 100 °C in a Safe-Lock Eppendorf tube at 800 rpm for 10 min in an Eppendorf shaker (Eppendorf) and subsequently stored at −20 °C for chemical analysis. Of selected N32-B, P21-A-pd, P22-B-pd and P40-B-pd digesta, an aliquot of 25 μL of the contents of the serum bottle containing some remaining RS-3 particles was used for SEM analyses (Section 2.6). The remaining contents in the serum bottles were washed with 0.75 mL sterile MQ twice and added to the Eppendorf tube containing the pellet, mixed and centrifuged once more (4 °C, 20,000 ×*g*, 10 min). The second supernatant was decanted and the Safe-Lock Eppendorf tubes containing the pellet were snap-frozen with liquid nitrogen, stored at −80 °C and freeze-dried. The times indicated in all figures are the inactivation times, except for t0; total sampling time took around 2–3 h.

2.3. Total starch quantification of fermented RS-3 preparations

Starch was quantified in the fermentation supernatants and pellets using the Megazyme Total Starch Kit (AA/AMG) (Megazyme, Wicklow, Ireland). For analysis of glucose + soluble starch in the supernatant, company protocol f was used, adjusted for smaller sample sizes. In short, the supernatant was defrosted and 50 μL was taken in duplicate. To each sample 50 μL 200 mM sodium acetate buffer pH 4.5 was added and incubated with 2 μL α-amylase (2500 U/mL on Ceralpha reagent at pH 5.0 and 40 °C, according to the company protocol) and 2 μL amyloglucosidase (3300 U/mL on soluble starch at pH 4.5 and 40 °C, according to the company protocol) at 50 °C for 30 min. The samples were further diluted with 100 mM sodium acetate buffer pH 5 to reach a final concentration of <0.8 mg/mL glucose.

To determine the total starch content in the initial RS-3 preparations, pre-digested RS-es and freeze-dried pellets after fermentation, approximately 500 μg sample was weighed in glass vials in duplicate using a microbalance (Mettler Toledo XP6 Microbalance, Columbus, Ohio, USA).

For pre-digested substrates and RS-3 preparations having a chain length > DPn 30, company protocol b was used, adjusted for smaller sample sizes. In short, 6 μL cold 80 % EtOH was added to 500 μg material and mixed. Next, 60 μL cold 1.7 M NaOH was added and mixed for 10 s. The mixture was stored on ice for 15 min while mixing multiple times. Subsequently, 240 μL 600 mM sodium acetate buffer pH 3.8 was added and mixed. Freeze-dried RS-3 preparations having a chain length < DPn 25 were hot-water soluble. Therefore, to the weighed samples obtained from these RS-3 preparations, 300 μL 100 mM sodium acetate buffer pH 4.5 was added and heated in a boiling water bath for 10 min to dissolve the starch. After dissolving the starch by either 1.7 M NaOH or by boiling, 250 μL was transferred to a new tube and 2 μL α-amylase (2500 U/mL) and 2 μL amyloglucosidase (3300 U/mL) were added. The samples were incubated at 50 °C for 30 min in an Eppendorf shaker (800 rpm) and 100 mM sodium acetate buffer pH 5 was added to obtain a final concentration of <0.8 mg/mL glucose.

Free glucose content was analysed with the GOPOD assay kit (Megazyme) using microtiter plates. Briefly, 15 μL diluted sample was added to a 96-well-plate in triplicate and 225 μL GOPOD reagents was added. A calibration curve of 0.1–0.8 mg/mL glucose was included in the analysis for quantification. The 96-well plates were incubated at 40 °C for 20 min and analysed with a Tecan Spectrophotometer at 520 nm (Tecan Infinite F500, Männedorf, Switzerland).

2.4. Molecular weight distribution of RS-3 remaining after fermentation

Freeze-dried pellets were solubilised in 1 M NaOH at 60 mg/mL sample. The samples were diluted to 2.5 mg/mL, to avoid re-precipitation of the linear α-1,4 glucans and neutralised by addition of 1 M HCl. The molecular weight distribution was analysed using HPSEC-RI according to Klostermann et al. (2021).

2.5. Short-chain fatty acids and organic acids produced by fermentation of RS-3 preparations

SCFAs, lactic and succinic acid were analysed as previously described (Kong et al., 2021). Samples were diluted 5 times with MQ and centrifuged at 19,000 ×*g* for 10 min. The supernatant (10 μL injection volume) was analysed using an Ultimate 3000 HPLC system (Dionex, Sunnyvale, California, USA) in combination with an Aminex HPX-87H column (Bio-Rad laboratories Inc., Hercules, California, USA). Acids were detected by a refractive index detector (RI-101, Shodex, Yokohama, Japan) and a UV detector set at 210 nm (Dionex Ultimate 3000 RS variable wavelength detector). Elution was performed at 0.5 mL/min and 50 °C using 50 mM sulphuric acid as eluent. Acetic, propionic, butyric, lactic and succinic acid standard curves were used for quantification (0.05–2 mg/mL). Data analysis was performed with Chromeleon™ 7.2.6 software from Thermo Fisher Scientific (Waltham, Massachusetts, USA).

2.6. Scanning electron microscopy of fermented RS-3 preparations

Fermented substrates N32-B, P21-A-pd, P22-B-pd and P40-B-pd were dried on 13 mm filters with 10 μm pores (Merck Isopore™ membrane filter (Merck, Burlington, Massachusetts, USA)), in a flow cabinet, attached to sample holders containing carbon adhesive tabs (EMS, Washington, USA) and sputter coated with 12 nm tungsten (EM SCD 500, Leica, Wetzlar, Germany). The samples were analysed using SEM (Magellan 400, FEI, Eindhoven, The Netherlands) at the Wageningen Electron Microscopy Center. SEM images were recorded at an acceleration voltage of 2 kV and 13 pA and magnification of 5000 (Everhart-Thornley detector), 10,000 and 25,000 (Through Lens Detector) times.

2.7. Microbiota composition analysis

DNA was extracted from approximately 1–10 mg of freeze-dried pellet followed by repeated bead-beating steps in Stool Transport and Recovery (STAR) buffer as previously described (Salonen et al., 2010). Afterwards, the DNA was purified using the Maxwell 16 Tissue LEV Total RNA Purification Kit Cartridge (XAS1220) (Promega, Madison, Wisconsin, USA). The purified DNA was diluted to 20 ng/μL using nuclease-free water.

Duplicate PCRs were performed using barcoded primers to amplify the V4 region of the 16S ribosomal RNA (rRNA) gene. The unique barcoded primer pair 515F (Parada, Needham, & Fuhrman, 2016) – 806R (Apprill, McNally, Parsons, & Weber, 2015) was used. Each PCR reaction contained 10 μL of 5× Phusion Green HF buffer (Thermo Fisher Scientific), 1 μL of 10 mM dNTPs (Promega), 0.5 μL of Phusion Hot start II DNA polymerase (2 U/μL) (Thermo Fisher Scientific), 1 μL of barcoded primers (10 μM) and 20 ng purified DNA. The reaction mixture was filled up with nuclease-free water to 50 μL (Qiagen, Hilden, Germany). The PCR program included an initial denaturation step for 30 s at 98 °C, followed by 25 cycles of 98 °C for 10 s, of 50 °C for 10 s and of 70 °C for 10 s, with a final extension of 70 °C for 7 min. For samples that had a DNA concentration < 20 ng/μL more DNA was added during PCR amplification or 30 PCR cycles were performed. The obtained PCR products were visualised on agarose gels, pooled and purified using CleanPCR (CleanNA, Waddinxveen, The Netherlands). The purified PCR products were quantified using the Qubit™ dsDNA BR assay kit (Invitrogen by Thermo Fisher Scientific) and a DeNovix DS-11 Fluorometer (DeNovix Inc., Wilmington, Delaware, USA). Two mock communities of known composition and one no-template control were included in each library. The PCR products were pooled in equimolar amounts and concentrated to 40 μL using CleanPCR. Libraries were sent for Illumina Hiseq2500 (2 × 150 bp) sequencing (Novogene, Cambridge, UK).

2.8. Data analysis

Raw sequence data of the 16S rRNA gene amplicons was processed using the NG-Tax 2.0 pipeline and default settings (Poncheewin et al., 2020). Taxonomy of each amplicon sequence variant (ASV) was assigned based on the SILVA database version 138.1 (Quast et al., 2013; Yilmaz et al., 2014). Data was analysed using R version 4.1.0, using the R packages phyloseq version 1.38.0 (McMurdie & Holmes, 2013), microbiome version 1.17.42 (Lahti & Shetty, 2012–2019) and microViz version 0.10.1 (Barnett, Arts, & Penders, 2021). Relative abundance of microbial taxa was calculated based on the 16S rRNA gene sequence read counts. Taxa that could not be identified at the genus level were renamed to the lowest classified taxonomic rank and sorted based on taxon abundance, *e.g.* the ASV of *Lachnospiraceae* Family 01 is the most abundant ASV of an unidentified genus within the *Lachnospiraceae*. The relative abundances of ASVs were visualised in a heatmap using the microViz package (Barnett et al., 2021). Principle component analysis (PCA) and principle coordinate analysis (PCoA) were used to visualise the microbiota variation between substrates after centered-log-ratio (CLR) transformation or Generalised UniFrac and Unweighted UniFrac distances, respectively. PERMANOVA analyses were performed to determine if physico-chemical characteristics of RS-3 significantly influenced the microbiota composition using the adonis function of the vegan package version 2.6.2 (Oksanen et al., 2022), and statistically different parameters were visualised by redundancy analyses using crystal type, Mw distribution (dispersity) and chain length as constraint variables. Statistical analyses on starch degradation and SCFA formation were not performed due to the limited number of biological replicates. The standard deviation obtained from biological duplicates is shown in the figures.

3. Results

3.1. Characteristics of RS-3 preparations

The *in vitro* fermentation studies were carried out using RS-3 preparations with known crystal type (A *vs.* B), chain length (DP16–76) and

Mw distribution (PI 1.07–2.11). These included six RS-3 substrates which were highly resistant (≥80 %) to pancreatic digestion (defined as "intrinsic RS-3") and two RS-3 preparations with lower resistance (20–70 %, defined as "RS-rich"). All RS-3 preparations were prepared previously and were described in detail by Klostermann et al. (2021). The most relevant physico-chemical characteristics of the eight RS-3 preparations are shown in Table 1. The sample names have been recoded compared to Klostermann et al. (2021) to improve intuitive understanding, with **N**: narrow disperse, **P**: polydisperse, **number**: DPn, **A**: A-type crystal, **B**: B-type crystal.

The intrinsic RS-3 preparations comprised of three substrates with an A-type crystal pattern (N16-A, N18-A, P21-A) and three with a B-type crystal pattern (N32-B, P53-B and N76-B). The intrinsic RS-3 preparations with an A-type crystal had a lower average Mw, compared to intrinsic RS-3 preparations with a B-type crystal (Table 1). The RS-rich RS-3 preparations comprised of two substrates with a B-type crystal, prepared from α-1,4 glucans of polydisperse Mw. These RS-3 preparations were partially pre-digested prior to fermentation to obtain an RS enriched fraction.

3.2. Fermentation of intrinsic RS-3 by adult gut microbiota

The six intrinsic RS-3 preparations were fermented *in vitro* during 48 h using an inoculum of a pool of four healthy adult faecal samples. After fermentation, the starch degradation and SCFA formation were quantified and the changes in microbiota composition were evaluated.

3.2.1. Intrinsic RS-3 substrates are degradable by adult gut microbiota

After incubation, the remaining insoluble and soluble starch fractions were quantified at given time points (Table S1; Table S2 for recoveries in substrate blanks). Up to 10 % of the intrinsic RS-3 preparations solubilised during incubation of intrinsic RS-3 preparations without inoculum. However, in the fermented intrinsic RS-3 substrates hardly any soluble starch was found, which indicates that fermentation of soluble starch was favoured over insoluble starch (Table S1).

Quantifying the remaining starch at different time points showed that all A-type intrinsic RS-3 substrates were fermented quite similarly (Fig. 1-A). N18-A was fermented slightly slower compared to N16-A and P21-A during the first 24 h, but its fermentation rate increased during the last 24 h of incubation. After 48 h, 65 % of all A-type intrinsic RS-3 preparations were degraded.

B-type intrinsic RS-3 preparations were fermented differently (Fig. 1-B). N32-B and N76-B (narrow disperse Mw distribution) were fermented at a very similar rate; after 24 h of fermentation the fermentation rate increased until around 65 % of the initial starch was fermented, similar to A-type intrinsic RS-3. The fermentation rate of P53-B (polydisperse Mw distribution) also increased after 24 h of fermentation, but after 48 h only 30 % of P53-B was fermented and thus final fermentability was lower compared to narrow disperse B-type intrinsic RS-3.

It should be noted that fully digestible starch was already almost completely fermented within 24 h (Table S1), whereas a maximum of 30 % of intrinsic RS-3 had been fermented within the same time frame. This indicates the slow fermentation of intrinsic RS-3, compared to digestible starch.

3.2.2. Intrinsic RS-3 preparations stimulate colonic butyrate production

To study the butyrogenic potential of intrinsic RS-3 substrates, SCFAs, lactic and succinic acid were quantified during the *in vitro* fermentation. In contrast to digestible starch, which showed high lactate production, intrinsic RS-3 substrates were mainly fermented to acetate and butyrate with only traces of propionate and lactate (<0.4 and <0.1 μmol/mg substrate, respectively) after 24 and 48 h of fermentation (Fig. 2), whereas no succinate was detected. As expected, very low concentrations of SCFAs were observed in the medium blanks (Fig. S1).

N16-A was fermented to acetate and butyrate in a ratio of ±2.7, illustrating a relatively high proportion of butyrate, at both 24 and 48 h of fermentation. N16-A was fermented to yield a total SCFA content of 7.0 μmol/mg substrate after 48 h of fermentation (Fig. 2-A). The acetate-butyrate ratio of N18-A was ±2.5 at 24 and 48 h of fermentation with a total SCFA content of 7.2 μmol/mg substrate (48 h). In contrast, fermentation of P21-A resulted in a decrease in the acetate-butyrate ratio from 3.0 to 1.5 after 24 and 48 h of incubation, respectively, with a total SCFA content of 5.5 μmol/mg substrate after 48 h of fermentation. P21-A (polydisperse Mw distribution) was thus fermented differently, compared to N16-A and N18-A (narrow disperse Mw distribution), although a rather similar amount of starch was utilised (Fig. 1-A).

Intrinsic RS-3 substrates with a B-type crystal pattern (N32-B, P53-B and N76-B) were mostly fermented to acetate and butyrate in an acetate-butyrate ratio of approximately 2.5 after 24 and 48 h, with a total SCFA content of 7.1, 5.0 and 6.8 μmol/mg substrate, respectively (Fig. 2-B). After 48 h, N76-B was fermented to acetate and butyrate in a ratio of 2.6 in one of the two duplicates, whereas a ratio of 1 was found in the other biological duplicate. The degradation of N76-B was similar for both biological duplicates (Fig. 1-B). These results indicate that the cross-feeding between the microbes was different in the two biological duplicates. P53-B was fermented to lower amounts of SCFAs (5.0 μmol/mg substrate at 48 h) compared to the other B-type intrinsic RS-3 substrates, which was in line with the higher starch recovery after fermentation (Fig. 1-B).

Overall, the intrinsic RS-3 substrates with a narrow disperse Mw

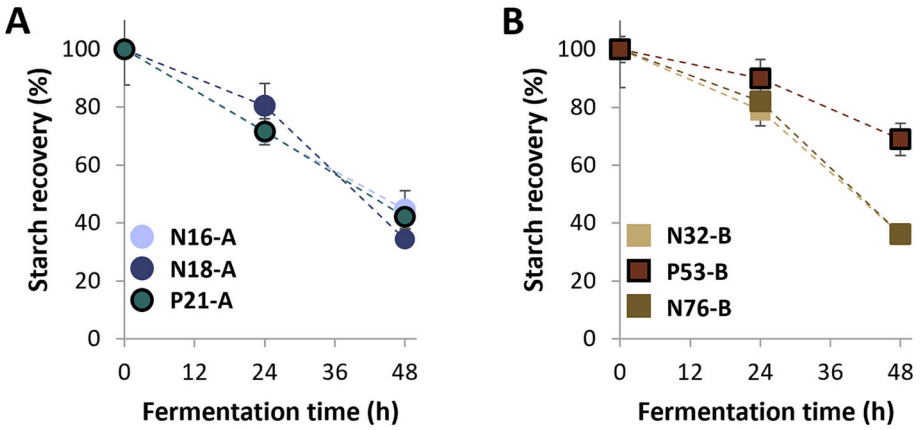

Fig. 1. Starch recovery after *in vitro* batch fermentation of intrinsic RS-3 with pooled adult faecal inoculum for 0, 24 and 48 h. Fig. A and B represent A-type and B-type intrinsic RS-3, respectively. All starch recovery values were normalised for starch recovery found at t0. Non-normalised starch recoveries can be found in Table S1. The average of biological duplicates is shown, including standard deviations. The error bars may be smaller than the marker used.

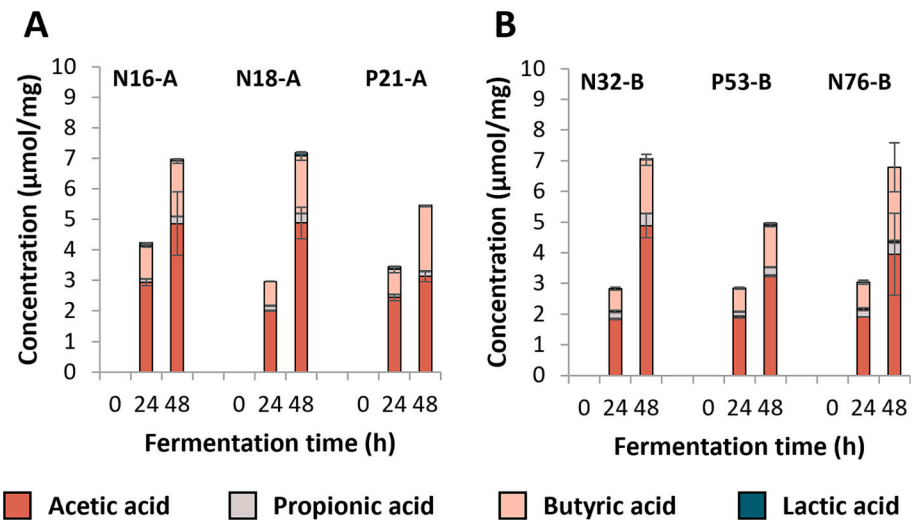

Fig. 2. SCFA and lactic acid formation (µmol/mg substrate) during 48 h of incubation of intrinsic RS-3 with pooled adult faecal inoculum. Fig. A and B represent A-type and B-type intrinsic RS-3, respectively. Results for the medium blank and positive control SPS are shown in Fig. S1. The average of biological duplicates is shown, including standard deviations.

distribution (N16-A, N18-A, N32-B and N76-B) were fermented to similar amounts of SCFAs (±7 µmol/mg substrate at 48 h) and a similar acetate-butyrate ratio (±2.5). In contrast, intrinsic RS-3 substrates with a polydisperse Mw distribution (P21-A and P53-B) were fermented to lower amounts of SCFAs (±5–5.5 µmol/mg substrate).

3.2.3. Intrinsic RS-3 preparations stimulate gut microbiota differently, depending on the physico-chemical characteristics

To study if intrinsic RS-3 preparations differing in crystal type, Mw and Mw distribution stimulated different microbial populations during fermentation, the microbiota composition over time was determined. Beta-diversity was determined after centered-log-ratio (CLR) transformation of relative abundances of ASVs (Fig. S2). CLR-PCA showed that the microbiota in t0 samples clearly separated from fermented intrinsic RS-3 and medium blanks, indicating that fermentation selectively stimulated microbial populations compared to the initial inoculum (Fig. S2). Independent of the intrinsic RS-3 physico-chemical characteristics, the same nine family level taxa covered >95 % of the relative abundance during all incubations (Fig. S3).

To have a more in-depth look on microbiota composition, we looked at ASVs explaining ≥2 % of the total relative abundance within an individual sample (medium blank or intrinsic RS-3) and together explaining ≥80 % of the total relative abundance at 24 or 48 h of fermentation (Fig. 3). Using the NCBI database we identified the ASVs further and found different species groups within obtained ASVs for *e.g. Bifidobacterium* and *Bacteroides* (Table S3). Within ASV *Bifidobacterium*

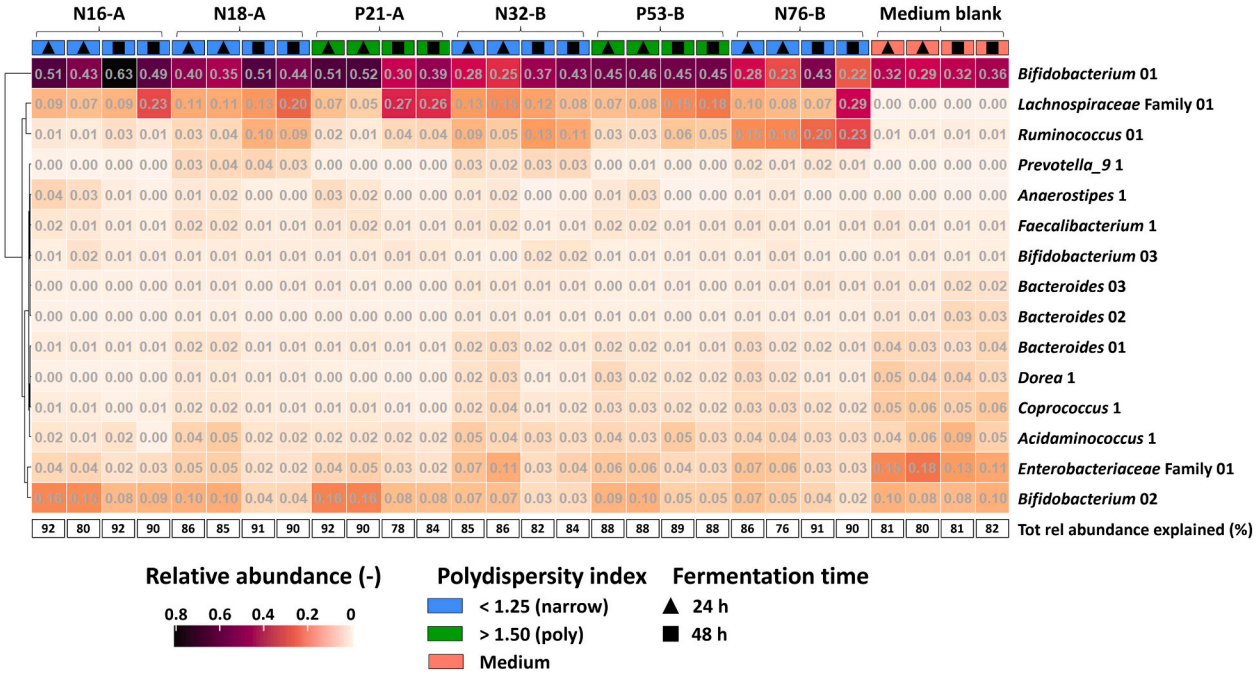

Fig. 3. Heatmap showing ASVs contributing ≥2 % to the total relative abundance within a sample, after 24 and 48 h of fermentation of intrinsic RS-3 and medium blank using pooled adult faecal inoculum. The cumulative relative abundance covered by these ASVs (%) is also provided. The taxa are sorted by hierarchical clustering of Euclidean distances.

01, we found a 100 % match with among others *B. adolescentis*, a primary degrader of RS in the gut (Ze et al., 2012). ASV *Ruminococcus* 01 had a 100 % match with key-stone RS degrader *R. bromii* (Ze et al., 2012) and recently discovered *Ruminococcoides bili* found in human bile (Molinero et al., 2021), for which RS degrading capability was proven as well.

In the heatmap, it is shown that around 80–90 % of the total relative abundance was explained by the same 15 ASVs for all samples, with *Bifidobacterium* 01, *Bifidobacterium* 02, *Lachnospiraceae* Family 01, and *Ruminococcus* 01 as the most dominant taxa (Fig. 3). *Bifidobacterium* 01 as well as *Bifidobacterium* 02 were present in all fermented intrinsic RS-3 substrates and medium blanks. Whereas *Bifidobacterium* 01 accounted for >20 % after 24 h of fermentation and increased in relative abundance to at least 30 % after 48 h of fermentation, the relative abundances of *Bifidobacterium* 02 were drastically lower. *Lachnospiraceae* Family 01 was present in all fermented intrinsic RS-3 substrates and varied between 5 and 15 % after 24 h of fermentation and increased to 9–29 % after 48 h of fermentation. This taxon was not present after fermentation in the medium blank without RS-3 and therefore is likely to be involved in the fermentation of intrinsic RS-3. It is noteworthy that the relative abundance of *Lachnospiraceae* Family 01 differed between biological duplicates of 48 h fermented N76-B (7 and 29 %) (Fig. 3), which could explain the differences found in SCFA ratio of this substrate (Fig. 2). *Ruminococcus* 01 was present for only 1–3 % in the fermented medium and most intrinsic RS-3 substrates, but specifically increased in relative abundance after fermentation of 1 A-type and two B-type

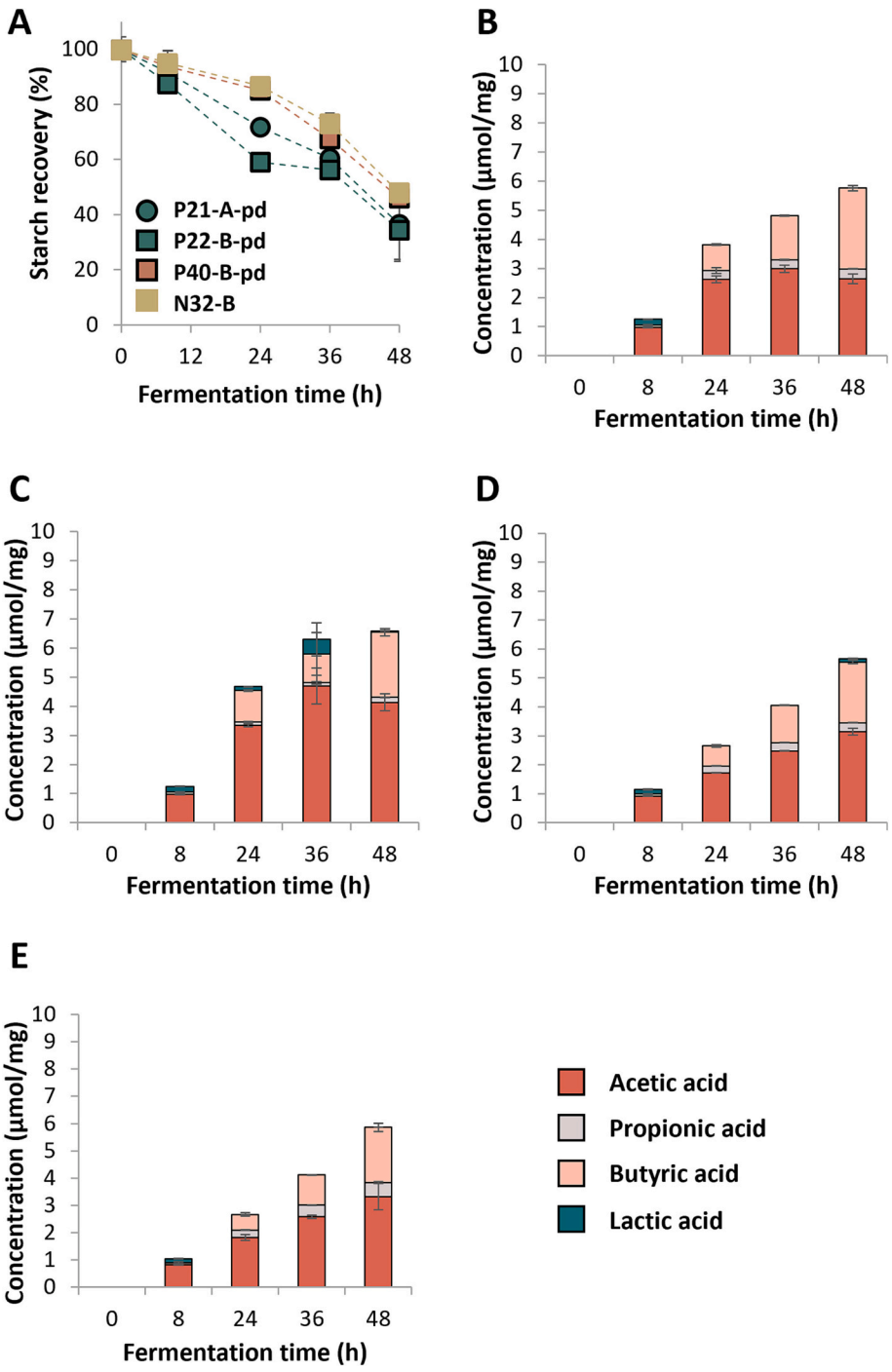

Fig. 4. A: Starch recovery during *in vitro* fermentation of pre-digested RS-3 preparations and N32-B using pooled adult faecal inoculum, normalised for starch recovery at t0. Non-normalised starch recoveries can be found in Table S4 and Table S5. Fig. B-E: SCFA and lactic acid formation (µmol/mg substrate) during 48 h of *in vitro* fermentation of P21-A-pd, P22-B-pd, P40-B-pd and N32-B, respectively. The average of biological duplicates is shown, including standard deviations. When standard deviations are not indicated, the standard deviations are smaller than the marker used.

intrinsic RS-3 substrates (N18-A, N32-B and N76-B), where it contributed for 10–20 % to the relative abundance (Fig. 3). For intrinsic RS-3 preparations N18-A and N32-B we also found 3–4 % *Prevotella_9* 1, which was absent in the medium blank and RS-3 substrates N16-A, P21-A and P53-B, indicating a minor role during fermentation of certain RS-3 substrates. Since *Lachnospiraceae* Family 01 and *Ruminococcus* 01 were dominant in the RS-3 incubations with neglectable growth in the medium blanks and showed co-occurring patterns across the incubations, we speculate that they are the primary fermenters of the RS-3 substrates.

3.3. Fermentation of pre-digested RS-rich RS-3 preparations

In vitro fermentation of intrinsic RS-3 showed that small differences in physico-chemical characteristics might impact the rate of starch degradation, SCFA production and microbiota composition. Most RS-3 preparations described in literature contain a digestible fraction and are thus not considered RS-3 directly. To study if the RS enriched fractions of RS-3 preparations that are rich in digestible starch showed similar microbial succession and activity compared to intrinsic RS-3 during *in vitro* fermentation, selected RS-3 preparations (P22-B and P40-B) were pre-digested and subsequently fermented *in vitro*. Their fermentability was compared to fermentation of intrinsic RS-3 N32-B and pre-digested intrinsic RS-3 P21-A, using the same conditions as used in Section 3.2. The starch degradation, SCFA and lactic acid formation (Fig. 4) and changes in microbiota composition (Fig. 5) during *in vitro* fermentation were evaluated.

All pre-digested RS-fractions were degraded for approximately 50–60 % within 48 h of fermentation, similarly to intrinsic RS-3 N32-B (Fig. 4-A). The fermentation rate of P21-A-pd and P22-B-pd was initially slightly faster than that of P40-B-pd and N32-B. The fermentation rate of P40-B-pd increased after 24 h of fermentation, similarly to N32-B. The microbial degradation of P21-A-pd, P22-B-pd and P40-B-pd did not influence the Mw distribution of the remaining substrate (Fig. S4).

SCFA analysis showed that all substrates were fermented to mostly acetate and butyrate during 48 h of fermentation (Fig. 4-B–E), irrespectively of starch degradation. During the first 8 h of incubation primarily acetate was formed, with minor amounts of lactate (<0.2 μmol/mg substrate), whereas butyrate was formed only from 24 h of fermentation onwards. The acetate-butyrate ratio after 48 h of fermentation was 1, 1.8, 1.5 and 1.6 for P21-A-pd, P22-B-pd, P40-B-pd and N32-B, respectively.

Fermented pre-digested RS-3 preparations showed the same nine family level taxa, covering >95 % of the relative abundance during all incubations (Fig. S5), similar to results obtained for intrinsic RS-3 (Fig. S3), but showing higher relative abundance of *Lachnospiraceae* across incubations.

The same 18 ASVs, contributing ≥2 % to the total relative abundance and together accounting for around 80–90 % of the total relative abundance, were found for all samples (Fig. 5) of which 13 ASVs were also found for fermentation of intrinsic RS-3 (Fig. 3). *Bifidobacterium* 01, *Bifidobacterium* 02, *Lachnospiraceae* Family 01, *Ruminococcus* 01 and *Enterobacteriaceae* Family 01 were the most dominant taxa present (Fig. 5). Relative abundance of *Bifidobacterium* 01 decreased between 24 and 48 h of fermentation for pre-digested RS-3 preparations, whereas relative abundance of *Lachnospiraceae* Family 01 increased from 2 to 12 % at 24 h to 13–44 % after 48 h. Relative abundance of *Ruminococcus* 01 increased in all fermented RS-3 substrates between 24 and 48 h, but was especially dominant in N32-B. Pre-digested RS-3 preparations P22-B-pd and P40-B-pd were thus fermented by slightly different microbial populations compared to intrinsic RS-3 N32-B. Especially for P21-A-pd, high relative abundance of *Lachnospiraceae* Family 01 was found, with an enormous increase between 24 and 48 h, similar to fermentation of P21-A without a pre-digestion treatment (Fig. 3). P21-A was fermented to the highest relative amount of butyrate among all fermentations, both when

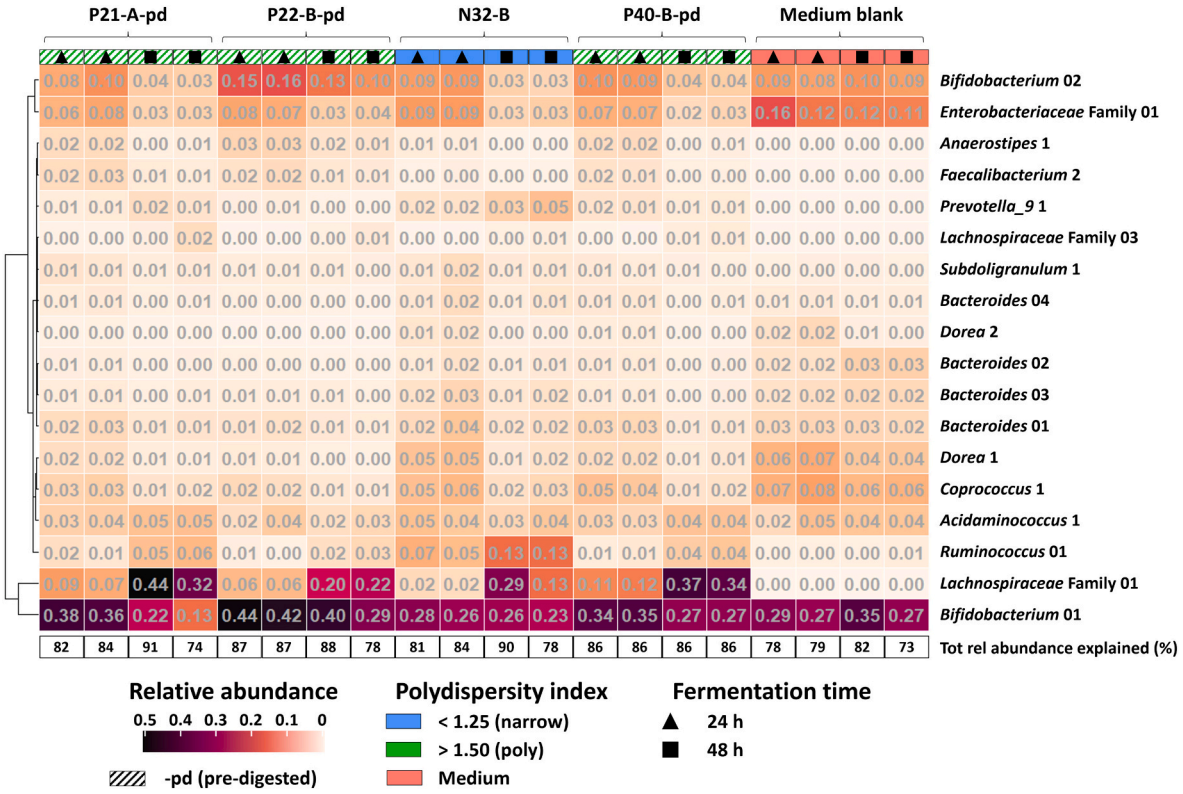

Fig. 5. Heatmap showing ASVs contributing ≥2 % to the total relative abundance within a sample after 24 and 48 h of fermentation of P21-A-pd, P22-B-pd, P40-pd, N32-B and medium blank using pooled adult faecal inoculum. The cumulative relative abundance covered by these ASVs (%) is also provided. The taxa are sorted by hierarchical clustering of Euclidean distances.

pre-digested or when used as such (Fig. 2-A, Fig. 4-B).

3.4. Pre-digested RS-3 fractions behave like intrinsic RS-3 during in vitro fermentation

To compare the RS enriched fractions of RS-rich RS-3 preparations with the intrinsic RS-3 substrates on microbiota composition during fermentation, β-diversities were determined after 24 and 48 h of incubation (Fig. S6) using CLR-transformation, Unweighted UniFrac and Generalised UniFrac distances. PERMANOVA analyses of Aitchison distances demonstrated that at 24 h of fermentation, crystal type explained 14.1 % ($P = 0.0038$) and Mw distribution explained 9.7 % of the variation ($P = 0.0319$) (Table S6). These parameters also approached significance using Unweighted UniFrac distances (P ~ 0.05), but using Generalised UniFrac only crystal type was significant, indicating that crystal type and Mw distribution affected the presence of certain taxa, whereas crystal type alone was significantly affecting the abundance of certain taxa. No taxa contributing ≥2 % of the total relative abundance (Fig. 3, Fig. 5) were observed that were absent in microbiota compositions of fermented RS-3 preparations differing in either Mw distribution or crystal type. This indicates that the variation explained by crystal type and Mw distribution using Unweighted UniFrac distances was due to presence or absence of taxa contributing ≤2 % of the total relative abundance within a sample.

At 48 h of fermentation, Mw distribution (dispersity) explained 12.3 % ($P = 0.0084$) and chain length explained 14.7 % of the variation ($P = 0.0035$) using Aitchison distances. These parameters were also significant using Unweighted UniFrac ($P \leq 0.01$) and Generalised UniFrac ($P < 0.05$) distances. To visualise the most significant parameters, redundancy analysis was performed on CLR-transformed microbial compositions at ASV level using crystal type and dispersity (24 h of fermentation) or dispersity and chain length (48 h of fermentation) as constraint variables (Fig. 6).

Although Mw distribution (dispersity) was not significantly affecting the abundance of certain taxa, the results show that at 24 h of fermentation, *Ruminococcus* 01 was associated with RS-3 preparations with a more narrow disperse Mw distribution (Fig. 6-A). This is in line with results presented in Fig. 3 and Fig. 5, where especially RS-3 preparations with a narrow Mw distribution overall showed a higher relative abundance of *Ruminococcus* 01. *Ruminococcus* 01 negatively correlated with *Faecalibacterium* 2 (Fig. 6-A), in line with results shown in Fig. 5. Furthermore, *Dorea* 1 was associated with RS-3 preparations with a B-type crystal, in line with results shown in Fig. 3 and Fig. 5, although this taxon was not among the most dominantly present taxa. At 48 h of fermentation, no clear associations between RS-3 physico-chemical parameters and taxa contributing ≥2 % to the total relative abundance were found (Fig. 6-B). In both plots, P22-B-pd seems to behave more like an A-type crystal, although it was confirmed that pre-digestion did not alter the crystal type (data not shown).

3.5. Visual degradation of RS-3 by adult gut microbiota

Since we observed different microbial populations associated with the different RS-3 physico-chemical characteristics and *Ruminococcus* 01

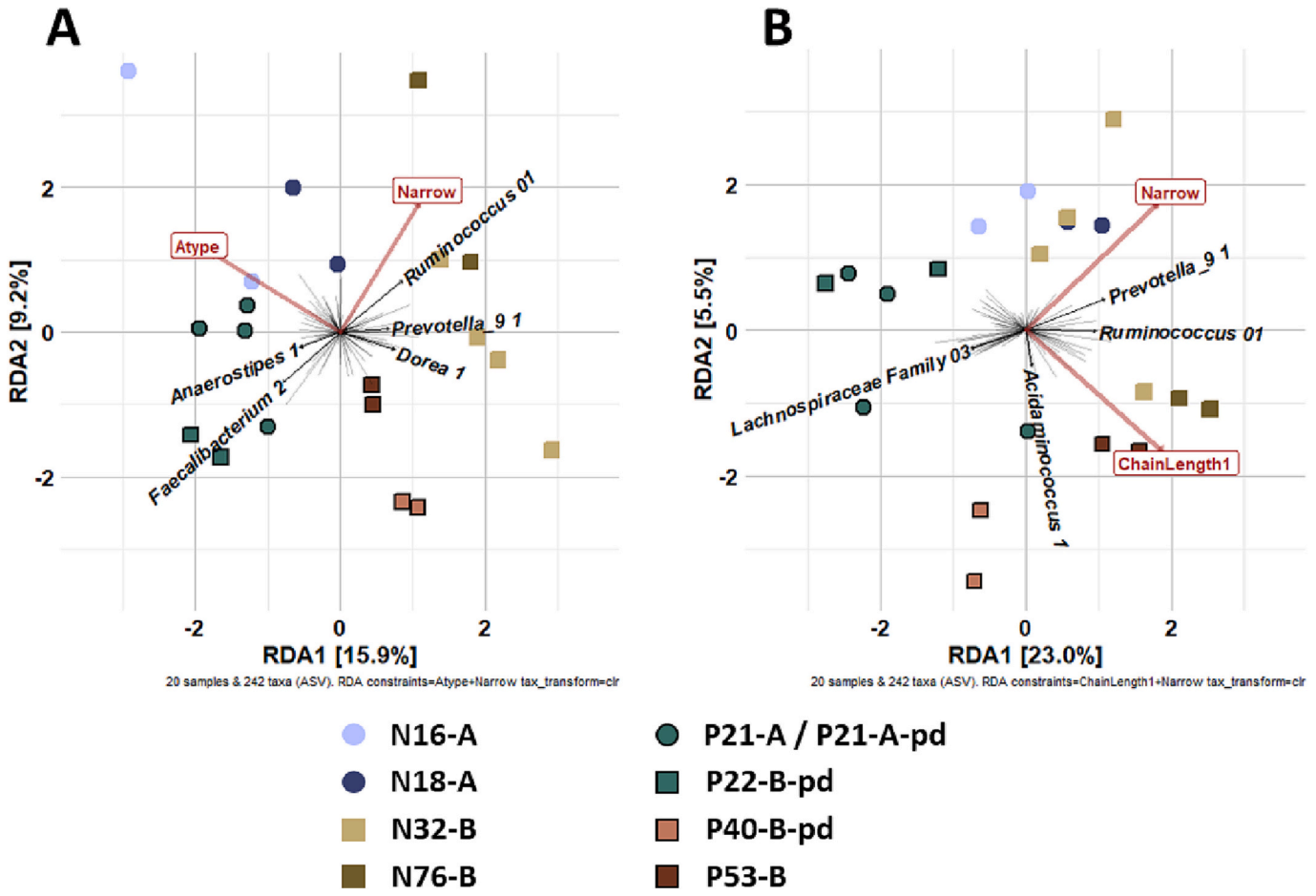

Fig. 6. RDA plots on CLR-transformed relative abundances of ASVs using physico-chemical parameters as constraint variables with A: Crystal type and dispersity at 24 h incubation and B: Chain length and dispersity at 48 h of incubation. Taxa shown contribute ≥2 % to the total relative abundance within a sample and contribute for >60 % relative to the largest taxa loadings within the RDA plot.

and *Lachnospiraceae* Family 01 as likely candidates for primary fermenters, we conducted SEM on N32-B, P21-A-pd, P22-B-pd and P40-B-pd to evaluate whether microbial populations attached to the RS-3 preparations and whether these populations differed among the RS-3 preparations.

The initial N32-B substrate consisted of quite regularly shaped spheres of around 5–7 μm (Fig. 7-A). Fig. 7-B and -C clearly show that over time the shape of the substrate changed and became less smooth. In addition, the surface of the substrate was dominantly attached by a coccus-shaped bacterium (Fig. 7-B, C), with an occasional presence of a rod-shaped bacterium (Fig. S7). Altogether, these results indicate that the N32-B substrate was degraded from the surface by coccus-shaped bacteria.

The SEM images of P21-A-pd and P22-B-pd show that these substrates consisted of tiny spheres that were connected to each other (Fig. 8-A1, B1). In contrast, P40-B-pd consisted of large chunks, without a clear microstructure (Fig. 8-C1). All pre-digested RS-3 preparations (polydisperse Mw distribution), had a very different structure than the regularly shaped and dense structure of N32-B (narrow disperse Mw distribution) (Fig. 7-A). The results show that after 24 h of fermentation rod-shaped bacteria attached to the pre-digested RS-3 substrates (Fig. 8-2), but also many non-degraded RS-3 particles were found. For P21-A-pd and P22-B-pd, still some untouched substrate was recognised after 48 h of fermentation, whereas for P40-B-pd, most chunks were covered by bacteria (Fig. S8). The rod-shaped bacteria seem to make holes within the substrates and hydrolyse/solubilise the RS-3 substrates from inside, irrespectively of crystal type or chain length.

Combining the SEM images after fermentation of N32-B and pre-digested RS-es (Fig. 7, Fig. 8), it becomes obvious that the degradation of these substrates by gut microbiota is different. Whereas rod-shaped bacteria were mostly attached to the RS-3 preparations with a polydisperse Mw distribution (Fig. 8), cocci were mostly attaching to RS-3 preparations with a narrow disperse Mw distribution (Fig. 7). Combined with our earlier observations on microbiota composition, we speculate that the coccus-shaped bacterium belongs to the *Ruminococcus* 01 taxon and the rod-shaped bacterium to *Lachnospiraceae* Family 01.

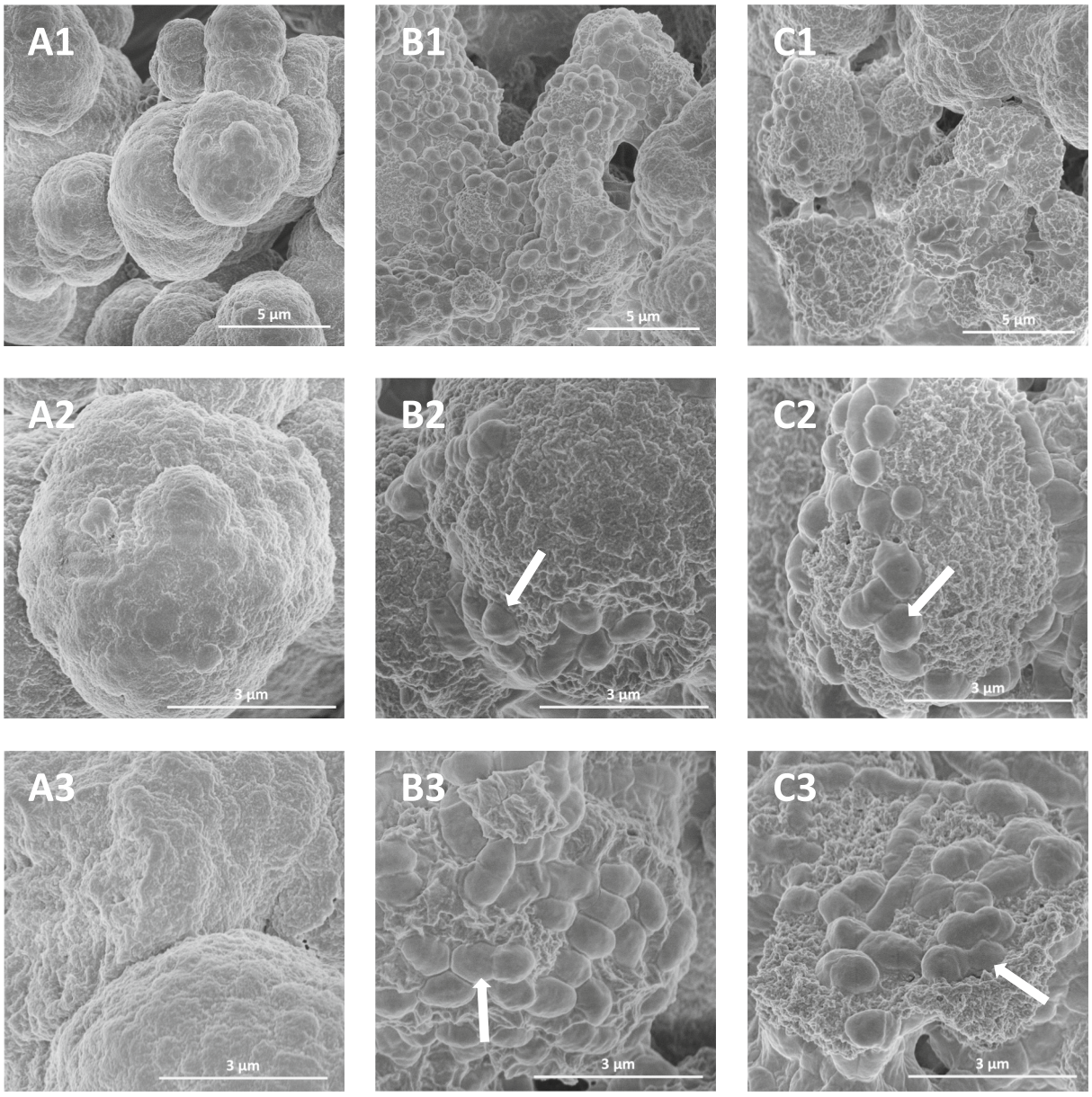

Fig. 7. SEM images of intrinsic RS-3 N32-B during fermentation. Fig. A, B and C represent N32-B blank and after 24 and 48 h of fermentation, respectively. Images 1 are 10,000 times magnified and images 2 and 3 are 25,000 times magnified. Arrows point towards the bacteria.

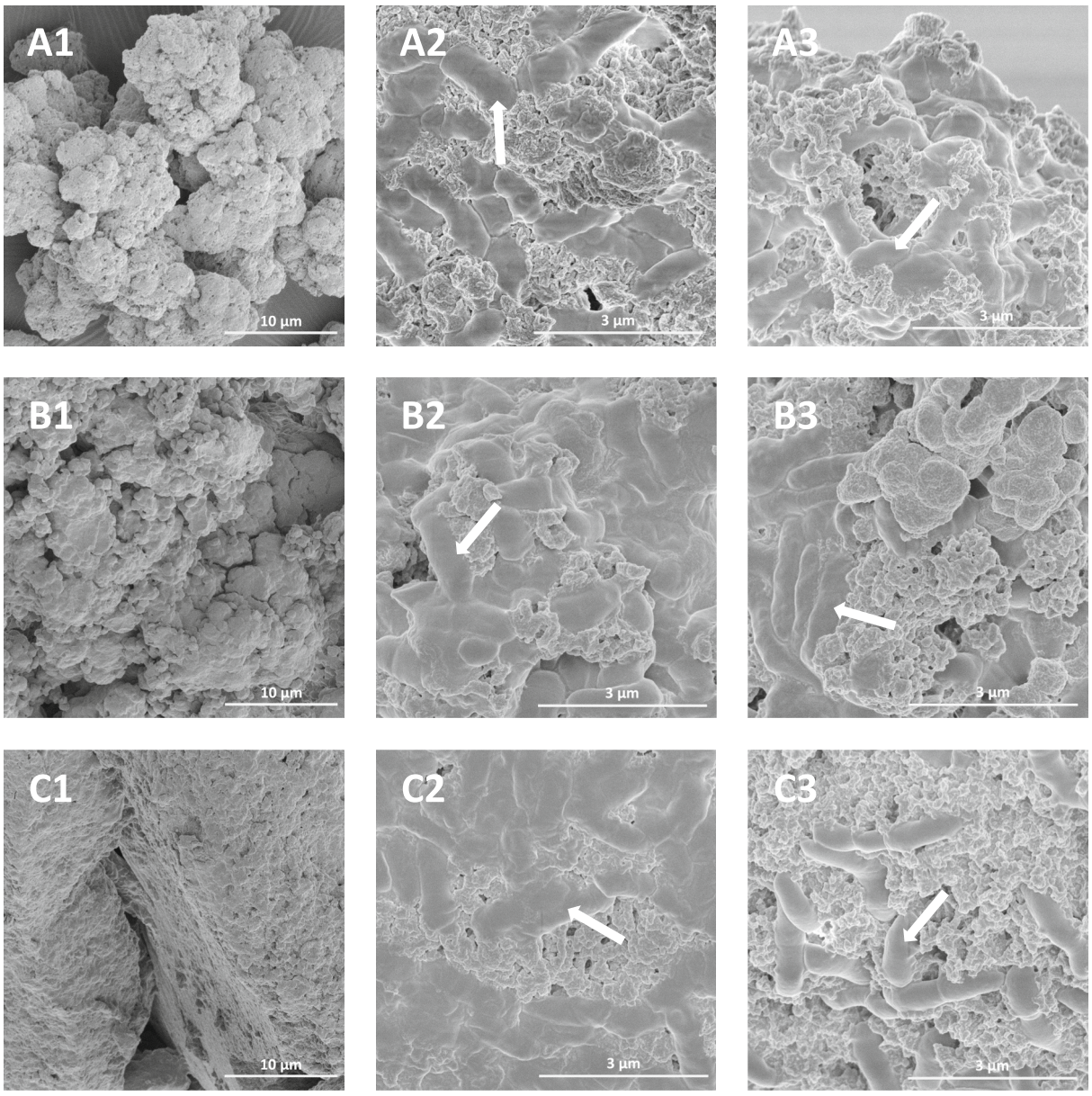

Fig. 8. SEM images of pre-digested RS-3 substrates (1), after 24 h of fermentation (2) and after 48 h of fermentation (3). A, B and C: P21-A-pd, P22-B-pd and P40-B-pd, respectively. Arrows highlight the presence of bacteria.

4. Discussion

Our results show that intrinsic RS-3 and pre-digested RS-rich RS-3 preparations were fermented slowly by gut microbiota (Fig. 1, Fig. 4-A). After 24 h of fermentation, no solubilised and hydrolysed starch was detected, indicating that hydrolysis of starch was more limiting than the conversion to SCFAs. Fermentation of intrinsic and pre-digested RS-3 stimulated the growth of bacteria belonging to the genera *Bifidobacterium*, *Lachnospiraceae* and *Ruminococcus*. Previously, it has already been shown that fermentation of RS-3 preparations increased the relative abundance of *Bifidobacterium* and *Lachnospiraceae* members (Teichmann & Cockburn, 2021). Fermentation of A- and B-type RS-3 preparations made of debranched waxy maize starch showed an increase in relative abundance of *Lachnospiraceae* members and *Prevotella*, but no distinct differences in microbial populations among fermented A- or B-type RS-3 preparations (Liu et al., 2022).

We found two different ASVs for *Bifidobacterium,* namely *Bifidobacterium* 01 and *Bifidobacterium* 02 (Fig. 3, Fig. 5). *Bifidobacterium* 01 was present for around 15 % in the initial inoculum and increased in all samples after fermentation to 20–60 % of the total relative abundance, whereas the relative abundance of *Bifidobacterium* 02 decreased between 24 and 48 h of fermentation of RS-3 substrates. The V4 region of *Bifidobacterium* 01 was 100 % identical to *B. adolescentis*, *B. faecale* and *B. dentium*, whereas the V4 region of *Bifidobacterium* 02 was 100 % identical to *B. pseudocatenulatum, B. longum* subsp. *longum, B. longum* subsp. *infantis*, *B. longum*, *B. breve* and *B. miconisargentati* (Table S3). Although all bifidobacteria mentioned encode genes for starch-degrading enzymes (Glycosyl Hydrolase family 13 (GH13); CAZy database (Drula et al., 2022)) and some have been shown to actively ferment starch (Belenguer et al., 2006; Ryan, Fitzgerald, & van Sinderen, 2006), only *B. adolescentis* is described as a primary degrader of RS (Dobranowski & Stintzi, 2021). *B. pseudocatenulatum* (covered by *Bifidobacterium* 02) has similar CBMs, including a raw starch-binding CBM74 (Valk, Lammerts van Bueren, van der Kaaij, & Dijkhuizen, 2016), and GH13 enzymes in its genome compared to *B. adolescentis* (CAZy (Drula et al., 2022)) and was shown to grow on cooked commercial RS-3 (Novelose®

330, ±50 % RS (Giuberti & Gallo, 2020)) (Baruzzi, de Candia, Quintieri, Caputo, & De Leo, 2017). Nevertheless, real RS-degrading capacities of this species have not yet been shown (Jung et al., 2019).

Whereas *Bifidobacterium* 01 increased in relative abundance in all fermented RS-3 substrates and the medium blank, *Ruminococcus* 01 only increased in some specific samples up to 20 % of the total relative abundance (Fig. 3, Fig. 5). The V4 region of *Ruminococcus* 01 was 100 % identical with *Ruminococcus bromii* and *Ruminococcoides bili*, according to NCBI Blast. From *R. bromii* it is known to be an RS degrading specialist (Ze et al., 2012), while also *R. bili,* isolated from human bile, was shown to be able to degrade a range of starches (Molinero et al., 2021).

The degradation rate during fermentation of N18-A, N32-B, N76-B (narrow disperse Mw distribution) increased after 24 h and especially during the last 24 h of incubation an increase in relative abundance of up to 20 % *Ruminococcus* 01 was found. Therefore, we speculate that *Ruminococcus* 01 was, at least partly, responsible for the degradation of N18-A, N32-B and N76-B. This hypothesis is strengthened by the recognition of mostly coccus-shaped bacteria after fermentation of intrinsic RS-3 N32-B, as shown by SEM images (Fig. 7). The degradation rate during fermentation of P40-B-pd and P53-B also increased during the last 24 h, but here we did not find such a pronounced increase in relative abundance of *Ruminococcus* 01. The degradation rate of N16-A, P21-A, P21-A-pd and P22-B-pd was very stable over time, stimulating mostly *Bifidobacterium* 01 and *Lachnospiraceae* Family 01. Although *Bifidobacterium* 01 matches with primary degrader *B. adolescentis*, it also increased in relative abundance in the medium blank, limiting us to speculate on primary degradation of these RS-3 preparations by *Bifidobacterium* 01. Since *Lachnospiraceae* specifically increased in relative abundance upon fermentation of RS-3, we speculate that N16-A, P21-A, P21-A-pd, P22-B-pd, P40-B-pd and P53-B (mostly polydisperse Mw distribution) were degraded by this bacterium, of which some members, such as *A. rectalis*, are recognised as secondary degraders of RS (Cerqueira et al., 2020; Cockburn, Cerqueira, Bahr, & Koropatkin, 2020). This hypothesis is strengthened by the presence of mostly rod-shaped bacteria after fermentation of P21-A-pd, P22-B-pd and P40-B-pd as visualised by SEM images (Fig. 8).

Our results showed that intrinsic RS-3 and pre-digested RS-rich RS-3 preparations were fermented to acetate and butyrate. Fermentation of RS-3 stimulated *Bifidobacterium* 01, *Ruminococcus* 01 and *Lachnospiraceae* Family 01. *Bifidobacterium* ferments its substrate to acetate and lactate (Pokusaeva et al., 2011), whereas *Lachnospiraceae* is known to harbour many butyrate producing genera (Meehan & Beiko, 2014; Vacca et al., 2020), of which some use lactate and acetate for their butyrate production (Duncan, Louis, & Flint, 2004). For all intrinsic RS-3 substrates, we found an increase in ASV *Lachnospiraceae* Family 01, but also *Faecalibacterium*, *Coprococcus* and *Anaerostipes,* present in lower relative abundance, might have contributed to the butyrate production *via* cross-feeding. The negative correlation found between *Ruminococcus* 01 and *Faecalibacterium* 02 (Fig. 6-A) can be explained by *R. bromii* degrading starch to malto-oligomers, maltose and accumulating glucose (Crost et al., 2018), whereas *F. prausnitzii* prefers to ferment acetate over glucose for the production of butyrate (Duncan et al., 2007). In contrast, enhanced butyrate production from starch was demonstrated by cross-feeding between *B. adolescentis* and *F. prausnitzii* previously (Rios-Covian, Gueimonde, Duncan, Flint, & de los Reyes-Gavilan, 2015). Especially butyrate production after fermentation of P21-A (polydisperse Mw distribution) was high, compared to intrinsic RS-3 with a narrow disperse Mw distribution. The acetate-butyrate ratio of fermented P21-A was also higher, compared to acetate-butyrate ratios found for RS-3 with an A-type crystal made from debranched waxy maize starch (Chang et al., 2021; Liu et al., 2022). Our study showed that small differences in physico-chemical characteristics of RS-3 influenced microbiota composition, and consequently butyrate production during fermentation. Also Gu et al. (2020) showed that RS-3 characteristics such as crystal type and chain length influenced the production of SCFAs and microbiota composition (Gu et al., 2020). Interestingly, our study showed that especially Mw distribution of the α-1,4 glucan chains is an important factor influencing microbiota composition and butyrate production.

5. Conclusions

Our study is the first to investigate the role of crystal type, Mw and Mw distribution towards the *in vitro* fermentability of RS-3 preparations by adult faecal microbiota. Tuning RS-3 physico-chemical characteristics slightly changed the microbiota composition and butyrate production during fermentation. Intrinsic RS-3 substrates were shown to be slowly fermentable fibres that stimulated *Lachnospiraceae*, *Ruminococcus* and *Bifidobacterium* phylotypes (ASVs) during *in vitro* fermentation. Especially the Mw distribution of α-1,4 glucans within RS-3 substrates influenced the relative abundance of *Lachnospiraceae* and *Ruminococcus* after fermentation. A more dense and homogeneous RS-3 microstructure, such as present in intrinsic RS-3 with a narrow disperse Mw distribution required RS-degrading specialists such as *Ruminococcus* for degradation, irrespectively of crystal type. In contrast, a less homogeneous RS-3 microstructure as present in RS-3 preparations with a polydisperse Mw distribution could potentially be degraded by dominantly present specific *Lachnospiraceae* ASVs. Especially A-type intrinsic RS-3 with a polydisperse Mw distribution yielded relatively high levels of butyrate. Due to the slow fermentation, intrinsic RS-3 will potentially arrive in the distal colon and have a beneficial effect for the host by promoting saccharolytic fermentation by potential probiotic bacteria stimulating butyrate production.

CRediT authorship contribution statement

C.E. Klostermann: Conceptualization, Methodology, Investigation, Writing – original draft. **M.F. Endika:** Investigation, Writing – review & editing. **E. ten Cate:** Methodology. **P.L. Buwalda:** Conceptualization. **P. de Vos:** Funding acquisition, Writing – review & editing. **J.H. Bitter:** Supervision, Writing – review & editing. **E.G. Zoetendal:** Writing – review & editing. **H.A. Schols:** Conceptualization, Supervision, Writing – review & editing.

Declaration of competing interest

The authors declare that they have no known competing financial interests or personal relationships that could have appeared to influence the work reported in this paper.

Data availability

Data will be made available on request.

Acknowledgements

This project is jointly funded by the Dutch Research Council (NWO), AVEBE, FrieslandCampina and Nutrition Sciences N.V. as coordinated by the Carbohydrate Competence Center (CCC-CarboBiotics; www.cccresearch.nl). The authors thank Ineke Heikamp – de Jong (WUR-MIB), Prof. dr. H. Smidt (WUR-MIB) and dr. L. Silva-Lagos (UMCG) for their contributions.

Appendix A. Supplementary data

Supplementary data to this article can be found online at https://doi.org/10.1016/j.carbpol.2023.121187.

References

Aguirre, M., Eck, A., Koenen, M. E., Savelkoul, P. H., Budding, A. E., & Venema, K. (2015). Evaluation of an optimal preparation of human standardized fecal inocula for in vitro fermentation studies. *Journal of Microbiological Methods, 117*, 78–84.

Apprill, A., McNally, S., Parsons, R., & Weber, L. (2015). Minor revision to V4 region SSU rRNA 806R gene primer greatly increases detection of SAR11 bacterioplankton. *Aquatic Microbial Ecology, 75*(2), 129–137.

Barnett, D. J. M., Arts, I. C. W., & Penders, J. (2021). microViz: An R package for microbiome data visualization and statistics. *Journal of Open Source Software, 6*(63), 3201.

Baruzzi, F., de Candia, S., Quintieri, L., Caputo, L., & De Leo, F. (2017). Development of a synbiotic beverage enriched with bifidobacteria strains and fortified with whey proteins. *Frontiers in Microbiology, 8*, 640.

Baxter, N. T., Schmidt, A. W., Venkataraman, A., Kim, K. S., Waldron, C., & Schmidt, T. M. (2019). Dynamics of human gut microbiota and short-chain fatty acids in response to dietary interventions with three fermentable fibers. *MBio, 10*(1).

Belenguer, A., Duncan, S. H., Calder, A. G., Holtrop, G., Louis, P., Lobley, G. E., & Flint, H. J. (2006). Two routes of metabolic cross-feeding between Bifidobacterium adolescentis and butyrate-producing anaerobes from the human gut. *Applied and Environmental Microbiology, 72*(5), 3593–3599.

Birt, D. F., Boylston, T., Hendrich, S., Jane, J. L., Hollis, J., Li, L., … Whitley, E. M. (2013). Resistant starch: Promise for improving human health. *Advances in Nutrition, 4*(6), 587–601.

Cai, L. M., & Shi, Y. C. (2014). Preparation, structure, and digestibility of crystalline A- and B-type aggregates from debranched waxy starches. *Carbohydrate Polymers, 105*, 341–350.

Cerqueira, F. M., Photenhauer, A. L., Pollet, R. M., Brown, H. A., & Koropatkin, N. M. (2020). Starch digestion by gut bacteria: Crowdsourcing for carbs. *Trends in Microbiology, 28*(2), 95–108.

Chang, R., Jin, Z., Lu, H., Qiu, L., Sun, C., & Tian, Y. (2021). Type III resistant starch prepared from debranched starch: Structural changes under simulated saliva, gastric, and intestinal conditions and the impact on short-chain tatty acid production. *Journal of Agricultural and Food Chemistry, 69*(8), 2595–2602.

Chen, J., & Vitetta, L. (2018). Inflammation-modulating effect of butyrate in the prevention of colon cancer by dietary fiber. *Clinical Colorectal Cancer, 17*(3), e541–e544.

Cockburn, D. W., Cerqueira, F. M., Bahr, C., & Koropatkin, N. M. (2020). The structures of the GH13_36 amylases from Eubacterium rectale and Ruminococcus bromii reveal subsite architectures that favor maltose production. *Amylase, 4*(1), 24–44.

Crost, E. H., Le Gall, G., Laverde-Gomez, J. A., Mukhopadhya, I., Flint, H. J., & Juge, N. (2018). Mechanistic insights into the cross-feeding of Ruminococcus gnavus and Ruminococcus bromii on host and dietary carbohydrates. *Frontiers in Microbiology, 9*, 2558.

Cushing, K., Alvarado, D. M., & Ciorba, M. A. (2015). Butyrate and mucosal inflammation: New scientific evidence supports clinical observation. *Clinical and Translational Gastroenterology, 6*, Article e108.

Dobranowski, P. A., & Stintzi, A. (2021). Resistant starch, microbiome, and precision modulation. *Gut Microbes, 13*(1), 1926842.

Drula, E., Garron, M. L., Dogan, S., Lombard, V., Henrissat, B., & Terrapon, N. (2022). The carbohydrate-active enzyme database: Functions and literature. *Nucleic Acids Research, 50*(D1), D571–D577.

Duncan, S. H., Holtrop, G., Lobley, G. E., Calder, A. G., Stewart, C. J., & Flint, H. J. (2007). Contribution of acetate to butyrate formation by human faecal bacteria. *British Journal of Nutrition, 91*(6).

Duncan, S. H., Louis, P., & Flint, H. J. (2004). Lactate-utilizing bacteria, isolated from human feces, that produce butyrate as a major fermentation product. *Applied and Environmental Microbiology, 70*(10), 5810–5817.

Fu, X., Liu, Z., Zhu, C., Mou, H., & Kong, Q. (2019). Nondigestible carbohydrates, butyrate, and butyrate-producing bacteria. *Critical Reviews in Food Science and Nutrition, 59*(sup1), S130–S152.

Giuberti, G., & Gallo, A. (2020). In vitro evaluation of fermentation characteristics of type 3 resistant starch. *Heliyon, 6*(1), Article e03145.

Gu, F., Li, C., Hamaker, B. R., Gilbert, R. G., & Zhang, X. (2020). Fecal microbiota responses to rice RS3 are specific to amylose molecular structure. *Carbohydrate Polymers, 243*, Article 116475.

Haralampu, S. G. (2000). Resistant starch - a review of the physical properties and biological impact of RS3. *Carbohydrate Polymers, 41*(3), 285–292.

Jacobasch, G., Dongowski, G., Schmiedl, D., & Muller-Schmehl, K. (2006). Hydrothermal treatment of Novelose 330 results in high yield of resistant starch type 3 with beneficial prebiotic properties and decreased secondary bile acid formation in rats. *British Journal of Nutrition, 95*(6), 1063–1074.

Jonathan, M. C., Borne, J. J., van Wiechen, P., da Silva, C. S., Schols, H. A., & Gruppen, H. (2012). In vitro fermentation of 12 dietary fibres by faecal inoculum from pigs and humans. *Food Chemistry, 133*(3), 889–897.

Jung, D. H., Kim, G. Y., Kim, I. Y., Seo, D. H., Nam, Y. D., Kang, H., … Park, C. S. (2019). Bifidobacterium adolescentis P2P3, a human gut bacterium having strong non-gelatinized resistant starch-degrading activity. *Journal of Microbiology and Biotechnology, 29*(12), 1904–1915.

Klostermann, C. E., Buwalda, P. L., Leemhuis, H., de Vos, P., Schols, H. A., & Bitter, J. H. (2021). Digestibility of resistant starch type 3 is affected by crystal type, molecular weight and molecular weight distribution. *Carbohydrate Polymers, 265*, Article 118069.

Kobayashi, K., Kimura, S., Naito, P. K., Togawa, E., & Wada, M. (2015). Thermal expansion behavior of A- and B-type amylose crystals in the low-temperature region. *Carbohydrate Polymers, 131*, 399–406.

Kong, C., Akkerman, R., Klostermann, C. E., Beukema, M., Oerlemans, M. M., Schols, H. A., & De Vos, P. (2021). Distinct fermentation of human milk oligosaccharides 3-FL and LNT2 and GOS/inulin by infant gut microbiota and impact on adhesion of *lactobacillus plantarum* WCFS1 to gut epithelial cells. *Food & Function, 12*(24), 12513–12525.

Lahti, R., & Shetty, S. (2012–2019). Microbiome r package: Tools for microbiome analysis in r. https://github.com/microbiome/microbiome [Accessed.2022].

Laverde Gomez, J. A., Mukhopadhya, I., Duncan, S. H., Louis, P., Shaw, S., Collie-Duguid, E., … Flint, H. J. (2019). Formate cross-feeding and cooperative metabolic interactions revealed by transcriptomics in co-cultures of acetogenic and amylolytic human colonic bacteria. *Environmental Microbiology, 21*(1), 259–271.

Li, L., Jiang, H. X., Kim, H. J., Yum, M. Y., Campbell, M. R., Jane, J. L., … Hendrich, S. (2015). Increased butyrate production during long-term fermentation of in vitro-digested high amylose cornstarch residues with human feces. *Journal of Food Science, 80*(9), M1997–M2004.

Liu, J., Liu, F., Arıoğlu-Tuncil, S., Xie, Z., Fu, X., Huang, Q., & Zhang, B. (2022). In vitro fecal fermentation outcomes and microbiota shifts of resistant starch spherulites. *International Journal of Food Science & Technology, 57*(5).

Maier, T. V., Lucio, M., Lee, L. H., VerBerkmoes, N. C., Brislawn, C. J., Bernhardt, J., … Jansson, J. K. (2017). Impact of dietary resistant starch on the human gut microbiome, metaproteome, and metabolome. *MBio, 8*(5).

Markiewicz, L. H., Ogrodowczyk, A. M., Wiczkowski, W., & Wroblewska, B. (2021). Phytate and butyrate differently influence the proliferation, apoptosis and survival pathways in human cancer and healthy colonocytes. *Nutrients, 13*(6).

Martens, B. M. J., Gerrits, W. J. J., Bruininx, E., & Schols, H. A. (2018). Amylopectin structure and crystallinity explains variation in digestion kinetics of starches across botanic sources in an in vitro pig model. *Journal of Animal Science and Biotechnology, 9*, 91.

McMurdie, P. J., & Holmes, S. (2013). phyloseq: An R package for reproducible interactive analysis and graphics of microbiome census data. *PLoS One, 8*(4), Article e61217.

McNabney, S. M., & Henagan, T. M. (2017). Short chain fatty acids in the colon and peripheral tissues: A focus on butyrate, colon cancer, obesity and insulin resistance. *Nutrients, 9*(12).

Meehan, C. J., & Beiko, R. G. (2014). A phylogenomic view of ecological specialization in the Lachnospiraceae, a family of digestive tract-associated bacteria. *Genome Biology and Evolution, 6*(3), 703–713.

Minekus, M., Smeets-Peeters, M., Bernalier, A., Marol-Bonnin, S., Havenaar, R., Marteau, P., … Huis in't Veld, J. H. (1999). A computer-controlled system to simulate conditions of the large intestine with peristaltic mixing, water absorption and absorption of fermentation products. *Applied Microbiology and Biotechnology, 53*(1), 108–114.

Molinero, N., Conti, E., Sánchez, B., Walker, A. W., Margolles, A., Duncan, S. H., & Delgado, S. (2021). Ruminococcoides bili gen. nov., sp. nov., a bile-resistant bacterium from human bile with autolytic behavior. *Internatiol Journal of Systematic and Evolutionary Microbiology, 71*(8), Article 004960.

Oksanen, J., Simpson, G. L., Kindt, R., Legendre, P., Minchin, P. R., O'Hara, R. B., … Weedon, J. (2022). *Package 'vegan'*.

Parada, A. E., Needham, D. M., & Fuhrman, J. A. (2016). Every base matters: Assessing small subunit rRNA primers for marine microbiomes with mock communities, time series and global field samples. *Environmental Microbiology, 18*(5), 1403–1414.

Plongbunjong, V., Graidist, P., Bach Knudsen, K. E., & Wichienchot, S. (2017). Starch-based carbohydrates display the bifidogenic and butyrogenic properties in pH-controlled faecal fermentation. *International Journal of Food Science & Technology, 52*(12), 2647–2653.

Pokusaeva, K., Fitzgerald, G. F., & van Sinderen, D. (2011). Carbohydrate metabolism in Bifidobacteria. *Genes & Nutrition, 6*(3), 285–306.

Poncheewin, W., Hermes, G. D. A., van Dam, J. C. J., Koehorst, J. J., Smidt, H., & Schaap, P. J. (2020). NG-Tax 2.0: A semantic framework for high-throughput amplicon analysis. *Frontiers in Genetics, 10*, 1366.

Pryde, S. E., Duncan, S. H., Hold, G. L., Stewart, C. S., & Flint, H. J. (2002). The microbiology of butyrate formation in the human colon. *FEMS Microbiology Letters, 217*(2), 133–139.

Quast, C., Pruesse, E., Yilmaz, P., Gerken, J., Schweer, T., Yarza, P., … Glockner, F. O. (2013). The SILVA ribosomal RNA gene database project: Improved data processing and web-based tools. *Nucleic Acids Research, 41*(Database issue), D590–D596.

Rios-Covian, D., Gueimonde, M., Duncan, S. H., Flint, H. J., & de los Reyes-Gavilan, C. G. (2015). Enhanced butyrate formation by cross-feeding between Faecalibacterium prausnitzii and Bifidobacterium adolescentis. *FEMS Microbiology Letters, 362*(21).

Ryan, S. M., Fitzgerald, G. F., & van Sinderen, D. (2006). Screening for and identification of starch-, amylopectin-, and pullulan-degrading activities in bifidobacterial strains. *Applied and Environmental Microbiology, 72*(8), 5289–5296.

Ryu, S. H., Kaiko, G. E., & Stappenbeck, T. S. (2018). Cellular differentiation: Potential insight into butyrate paradox? *Molecular & Cellular Oncology, 5*(3), Article e1212685.

Salonen, A., Nikkila, J., Jalanka-Tuovinen, J., Immonen, O., Rajilic-Stojanovic, M., Kekkonen, R. A., … de Vos, W. M. (2010). Comparative analysis of fecal DNA extraction methods with phylogenetic microarray: Effective recovery of bacterial and archaeal DNA using mechanical cell lysis. *Journal of Microbiological Methods, 81*(2), 127–134.

Scheiwiller, J., Arrigoni, E., Brouns, F., & Amado, R. (2006). Human faecal microbiota develops the ability to degrade type 3 resistant starch during weaning. *Journal of Pediatric Gastroenterology and Nutrition, 43*(5), 584–591.

Teichmann, J., & Cockburn, D. W. (2021). In vitro fermentation reveals changes in butyrate production dependent on resistant starch source and microbiome composition. *Frontiers in Microbiology, 12*, Article 640253.

Vacca, M., Celano, G., Calabrese, F. M., Portincasa, P., Gobbetti, M., & De Angelis, M. (2020). The controversial role of human gut Lachnospiraceae. *Microorganisms, 8*(4).

Valk, V., Lammerts van Bueren, A., van der Kaaij, R. M., & Dijkhuizen, L. (2016). Carbohydrate-binding module 74 is a novel starch-binding domain associated with large and multidomain alpha-amylase enzymes. *FEBS Journal, 283*(12), 2354–2368.

Wang, M., Wichienchot, S., He, X., Fu, X., Huang, Q., & Zhang, B. (2019). In vitro colonic fermentation of dietary fibers: Fermentation rate, short-chain fatty acid production and changes in microbiota. *Trends in Food Science & Technology, 88*, 1–9.

Yilmaz, P., Parfrey, L. W., Yarza, P., Gerken, J., Pruesse, E., Quast, C., … Glockner, F. O. (2014). The SILVA and "all-species living tree project (LTP)" taxonomic frameworks. *Nucleic Acids Research, 42*(Database issue), D643–D648.

Ze, X., Duncan, S. H., Louis, P., & Flint, H. J. (2012). Ruminococcus bromii is a keystone species for the degradation of resistant starch in the human colon. *The ISME Journal, 6*(8), 1535–1543.

Zhang, C., Qiu, M., Wang, T., Luo, L., Xu, W., Wu, J., Zhao, F., Liu, K., Zhang, Y., & Wang, X. (2021). Preparation, structure characterization, and specific gut microbiota properties related to anti-hyperlipidemic action of type 3 resistant starch from Canna edulis. *Food Chemistry, 351*, Article 129340.

Zhou, Z., Cao, X., & Zhou, J. Y. H. (2013). Effect of resistant starch structure on short-chain fatty acids production by human gut microbiota fermentation in vitro. *Starch-Starke, 65*(5–6), 509–516.